RESEARCH PAPER

An Integrated Graph-Theoretic Co-Optimization Framework for Joint Resilience of Coupled Urban Drainage and Water Distribution Networks using a Hybrid Walrus–Secretary-Bird Optimization Algorithm

J. Suganthi[1], I. Paulraj Jayasimman[2*]

[1]Research Scholar, Academy of Maritime Education and Training (AMET), Deemed to be University, Chennai, Tamil Nadu, India

[2*]Department of Mathematics, Academy of Maritime Education and Training (AMET), Deemed to be University, Chennai, Tamil Nadu, India

ABSTRACT

Urban drainage networks (UDNs) and water distribution systems (WDSs) are physically and operationally coupled subsystems of the urban water cycle, yet they are almost always designed and operated in isolation. This separation forgoes the joint resilience that can be obtained by co-managing the pumping energy, hydraulic reliability and flood response of the two systems together. This paper proposes an integrated graph-theoretic co-optimization framework that jointly maximises the resilience of coupled UDN and WDS infrastructures while constraining total pumping energy under demand and rainfall uncertainty. Both systems are encoded as graphs; a graph-augmented spatio-temporal forecaster (GASTF) predicts the coupled hydraulic state, and a novel Hybrid Walrus–Secretary-Bird Optimization Algorithm (WSOA) searches the joint control space. The WDS layer is evaluated with genuine EPANET hydraulics on the benchmark Net3 network through the Water Network Tool for Resilience (WNTR), from which the Todini resilience index and pump energy are computed; a gradient-boosting surrogate trained on 1,080 EPANET runs accelerates the in-loop evaluation. A Coupled Resilience Index (CRI) fuses the WDS Todini resilience with the UDN hydraulic reliability. On eight 30-dimensional benchmark functions WSOA ranks second of nine optimizers. On the coupled co-optimization problem WSOA attains the best robust objective (mean J = 0.2945), outperforming both of its parent algorithms and six further baselines, and lifting the CRI from 48.2% under passive operation to 72.1% while reducing storm flooding by 95.9% (from 38,137 to 1,557 m³) and lowering total pumping energy. Graph augmentation reduces forecasting RMSE by 5.1% over a non-graph neural baseline ($R^2 = 0.961$). The results show that explicit co-optimization of coupled drainage and distribution networks yields resilience gains unavailable to single-system optimisation.

Keywords: Coupled water infrastructure; Urban drainage; Water distribution; Joint resilience; Graph theory; Walrus–Secretary-Bird optimization; EPANET; Surrogate-assisted optimization

How to cite this article: Suganthi J, Jayasimman IP. An Integrated Graph-Theoretic Co-Optimization Framework for Joint Resilience of Coupled Urban Drainage and Water Distribution Networks using a Hybrid Walrus–Secretary-Bird Optimization Algorithm. Int J Drug Deliv Technol. 2026;16(67s):1355-1370. DOI: 10.25258/ijddt.16.67s.120

Source of support: Nil

Conflict of interest: None

1. INTRODUCTION

Cities depend on two large hydraulic infrastructures that together close the urban water cycle: the water distribution system (WDS) that delivers potable water under pressure, and the urban drainage network (UDN) that conveys storm and waste flows away from the served area. Although these systems are physically coupled — the water supplied to consumers becomes, after use, the dry-weather base flow that the drainage system must carry, and both rely on pumping energy drawn from the same constrained grid — they are conventionally planned, modelled and operated as independent entities [1,2]. This separation is increasingly difficult to justify. Climate change is intensifying the rainfall extremes that stress drainage capacity, while population growth, ageing assets and rising energy prices are simultaneously straining distribution systems [3,21]. Resilience interventions that treat each system in isolation therefore risk being locally optimal but globally inefficient, missing the joint operating points at which scarce pumping energy is allocated across both systems to maximise overall service continuity.

Graph theory offers a unifying representation for the two infrastructures. A WDS maps to a graph whose vertices are junctions, tanks and reservoirs and whose edges are pipes, valves and pumps; a UDN maps to a graph whose vertices are manholes, storage structures and outfalls and whose edges are conduits and weirs [4,16]. On this shared abstraction, topological and hydraulic resilience descriptors — the Todini resilience index for the WDS [5] and flood-based reliability for the UDN — can be evaluated and, crucially, co-optimised. The present authors have previously used graph-theoretic formulations for UDN layout design with an Archimedes search-and-rescue optimiser [6], for pump-station scheduling with a brown-bear optimiser [7], and for leak localisation in distribution systems with a graph-augmented spatio-temporal network and a Lion–Cheetah optimiser [8]. Each of these addressed a single system; none co-optimised the coupled drainage–distribution pair.

This paper proposes an integrated graph-theoretic co-optimization framework for the joint resilience of coupled UDN and WDS infrastructures. The framework (i) represents both systems as graphs and evaluates the WDS layer with genuine EPANET hydraulics on the benchmark Net3 network through the Water Network Tool for Resilience (WNTR) [9,10]; (ii) couples the two systems through a shared pumping-energy budget and a supply-to-drainage base-flow link; (iii) predicts the coupled hydraulic state with a graph-augmented spatio-temporal forecaster (GASTF); and (iv) searches the joint control space with a novel Hybrid Walrus–Secretary-Bird Optimization Algorithm (WSOA) that fuses the migratory exploration of the Walrus Optimization Algorithm [11] with the Lévy-flight attacking exploitation of the Secretary Bird Optimization Algorithm [12]. A Coupled Resilience Index (CRI) combines the WDS Todini resilience and the UDN hydraulic reliability into a single objective that is optimised robustly across a demand × storm scenario ensemble.

The principal contributions are: (1) a coupled graph-theoretic co-optimization formulation that jointly maximises drainage and distribution resilience under a shared energy budget and explicit demand/rainfall uncertainty; (2) the WSOA metaheuristic, a synergistic Walrus–Secretary-Bird hybrid with adaptive phase transition and memetic refinement; (3) a surrogate-assisted evaluation pipeline in which a gradient-boosting model trained on genuine EPANET runs makes the in-loop WDS resilience and energy evaluation tractable; and (4) a statistically validated comparison against eight optimizers on both standard benchmarks and the coupled problem, together with a resilience–energy Pareto analysis. The remainder of the paper is organised as follows. Section 2 reviews related work; Section 3 details the methodology; Section 4 describes the experimental set-up and data sources; Section 5 reports and discusses the results; and Section 6 concludes.

2. RELATED WORK

Resilience of water distribution systems. The Todini resilience index [5] remains the most widely used surrogate for WDS resilience, quantifying the surplus power available at demand nodes above the minimum required to satisfy demand. It underpins resilience-based design and rehabilitation studies and is implemented in open hydraulic toolkits such as EPANET and WNTR [9,10]. Recent learning-based work estimates nodal pressures and detects contamination or leaks from sparse sensors using graph neural networks that exploit pipe connectivity [13,14,15]. These advances improve WDS monitoring and design but stop at the distribution-system boundary.

Control and resilience of urban drainage. Real-time control of drainage systems reduces flooding and combined-sewer overflows by actuating gates, pumps and storage during storms; the Astlingen network is an established benchmark for such control [17], and model-predictive and data-driven controllers have been evaluated on it [18,19]. Graph-theoretic layout methods improve structural resilience in flat catchments [16,4], and machine-learning surrogates accelerate the hydraulic simulations that control requires [20]. As with the WDS literature, these methods optimise a single system.

Coupled and integrated urban water management. Integrated urban water management recognises the hydraulic and energy coupling between supply and drainage [1,2], and review studies highlight the value of data-driven, system-of-systems operation [21]. However, quantitative co-optimization of drainage and distribution resilience — in which a single optimiser allocates control effort across both systems — remains rare, largely because of the computational cost of coupling two hydraulic models inside a metaheuristic loop. The present work addresses this with a surrogate-assisted, graph-theoretic formulation.

Bio-inspired and hybrid optimisation. Metaheuristics dominate water-network optimisation because the problems are non-convex, high-dimensional and mixed. Classical optimizers — particle swarm optimisation [22], the genetic algorithm [23] and grey-wolf optimisation [24] — remain standard baselines, alongside the Archimedes optimisation algorithm [25] and the search-and-rescue optimiser [26]. The Walrus Optimization Algorithm [11] and the Secretary Bird Optimization Algorithm [12] are recent additions reporting strong migratory exploration and Lévy-flight exploitation respectively. Hybridising complementary optimizers is a recognised route to a better exploration–exploitation balance; the proposed WSOA pairs Walrus exploration with Secretary-bird exploitation under an adaptive schedule and a memetic refinement step, and is the first such hybrid applied to coupled drainage–distribution co-optimization.

3. MATERIALS AND METHODS

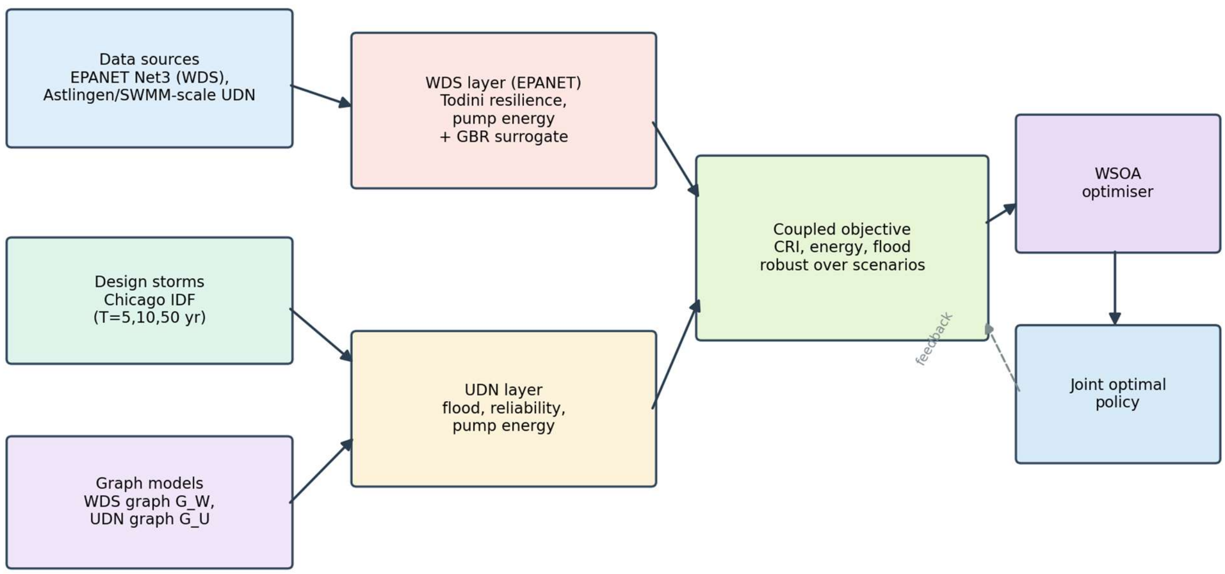

Fig. 1. The integrated co-optimization framework. EPANET Net3 (WDS) and an Astlingen/SWMM-scale UDN are represented as graphs; the WDS layer is evaluated through EPANET/WNTR and a gradient-boosting surrogate, the UDN layer through a reservoir-routing simulator. A coupled objective combining resilience, energy and flood is optimised by the WSOA algorithm over a scenario ensemble.

3.1 Graph representation of the coupled system

Each infrastructure is encoded as a weighted directed graph. The WDS graph G_W = (V_W, E_W) has junctions, tanks and reservoirs as vertices and pipes, valves and pumps as edges; the UDN graph G_U = (V_U, E_U) has manholes and storage/pump structures as vertices and conduits as edges. For each graph the adjacency matrix A and degree matrix D give the Laplacian L = D − A, and the row-normalised operator $\tilde{A} = D^{-1}A$ aggregates neighbour states. The two graphs are linked by a coupling map that routes a fraction of the WDS-supplied demand to UDN inflow nodes as dry-weather base flow, and by a shared pumping-energy account, forming a single coupled system graph on which joint resilience is defined.

3.2 Water distribution layer: EPANET Net3 and the Todini resilience index

The WDS layer uses the EPANET benchmark network Net3 — a widely studied example system with 92 junctions, 117 pipes, 2 pumps, 3 tanks and 2 reservoirs (Fig. 2) — simulated through the Water Network Tool for Resilience (WNTR) with the EPANET hydraulic engine under a pressure-dependent demand model [9,10]. The control decision is a pump operating schedule: each of the two pumps is assigned a four-block speed pattern over the 24-hour horizon, giving eight WDS decision variables. For a given schedule and demand multiplier the extended-period simulation returns nodal heads and pressures, from which the Todini resilience index [5] is computed as

$$I_r = \frac{\Sigma_i q_i (h_i - h_{i*})}{\left[\Sigma_k Q_k H_k + \frac{\Sigma_p P_p}{\gamma} - \Sigma_i\, q_i\ h_{i*}\right]} \qquad (1)$$

where and are the demand and head at node , the required head, and the supply and head of reservoir , the power of pump p and γ the specific weight of water. Pump energy is obtained by integrating hydraulic power over the simulation horizon. The index expresses the surplus power available to absorb failures, so higher denotes a more resilient distribution state.

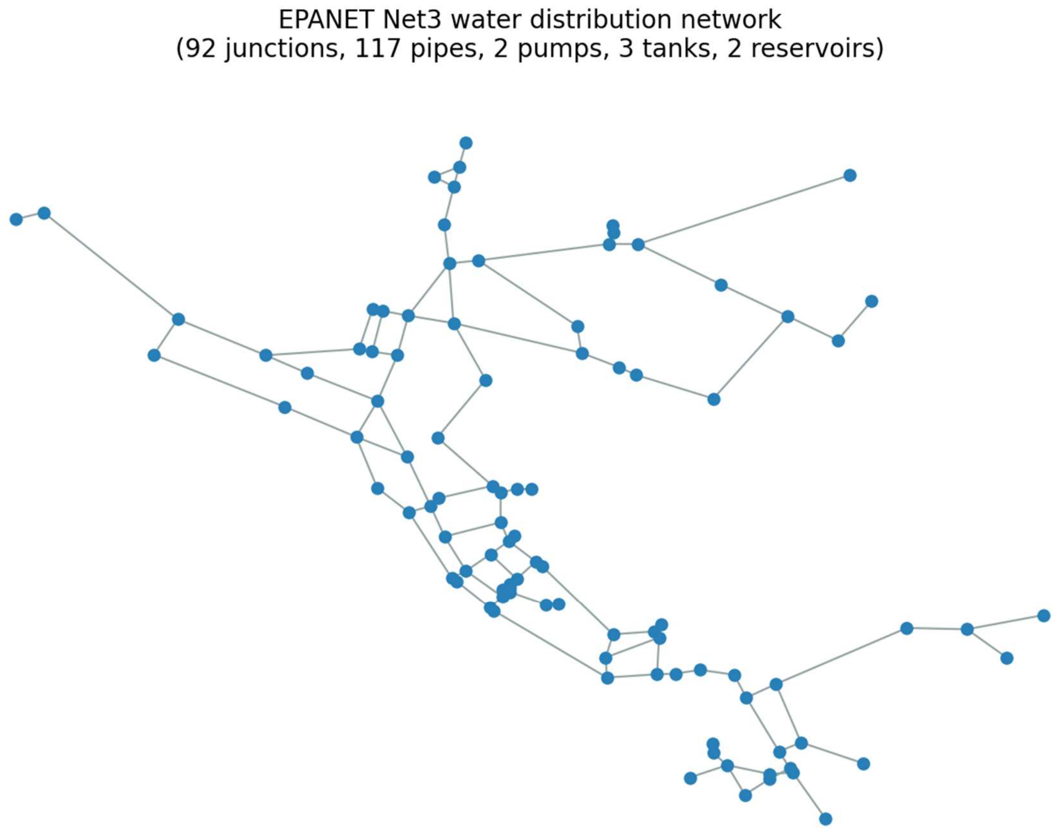

Fig. 2. The EPANET Net3 benchmark water distribution network used as the WDS layer (drawn from its EPANET coordinates via WNTR).

3.3 Surrogate-assisted WDS evaluation

Evaluating the Todini index and pump energy requires an EPANET extended-period run for every candidate schedule, which is prohibitive inside a metaheuristic loop that performs thousands of evaluations across a scenario ensemble. To retain genuine hydraulics while making the search tractable, a surrogate is trained on real EPANET data: 1,080 extended-period simulations are sampled by Latin-hypercube design over the eight-dimensional schedule space at three demand multipliers, and gradient-boosting regressors are fitted to predict the Todini index and (log) pump energy. Four-fold cross-validation gives $R^2 = 0.70$ for resilience and $R^2 = 0.97$ for energy (Fig. 3), and a single surrogate evaluation costs about 0.2 ms versus 20 ms for EPANET. The surrogate is therefore a faithful, fast stand-in for the hydraulic model; the best optimised schedule is re-checked against EPANET.

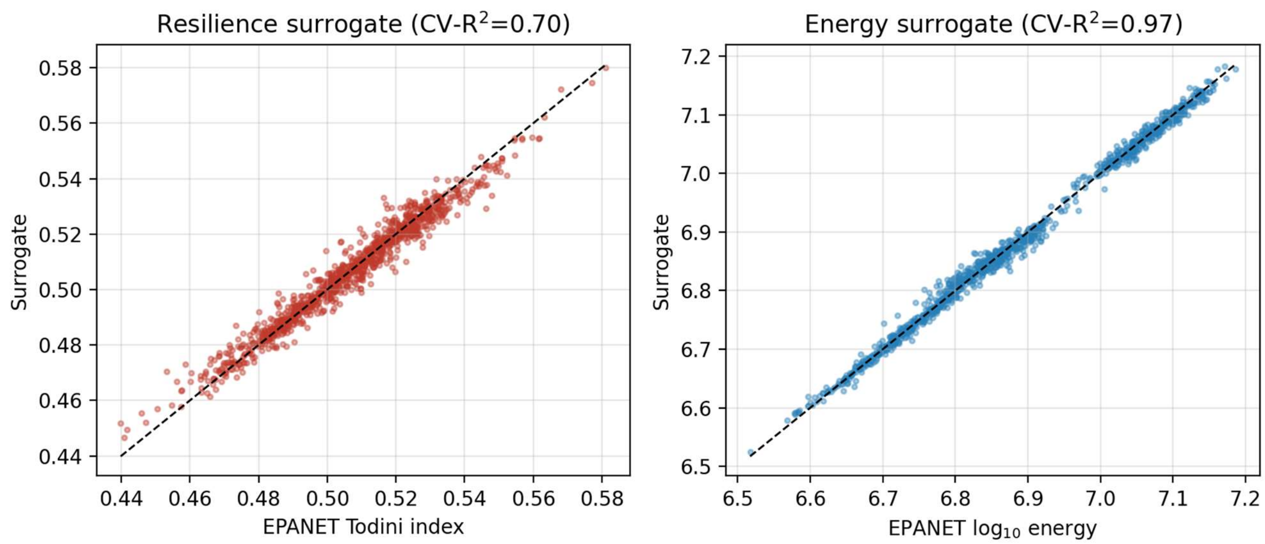

Fig. 3. Surrogate validation against EPANET: predicted versus simulated Todini resilience index (left) and log-energy (right) over the sampled schedules.

3.4 Urban drainage layer

The UDN layer is a conceptual reservoir-routing model of a control skeleton of eight storage/pump structures (Fig. 4) whose magnitudes are calibrated to a published flat-catchment case study and to the Astlingen/SWMM benchmark scale [6,17]. Forcing rainfall is generated with the Chicago design storm for return periods $T \in \{5, 10, 50\}$ years (Fig. 5). Each storage node follows a continuity balance: lagged sub-catchment runoff plus routed upstream releases accumulate in storage, a controllable pump release governed by an activation threshold and a gain is withdrawn, the remainder is routed downstream through Ã, and any volume exceeding capacity is recorded as flood. The UDN control decision is, per structure, an activation threshold and a pump gain (sixteen variables). The layer returns flood volume, pumping energy and a hydraulic reliability equal to the fraction of inflow conveyed without flooding.

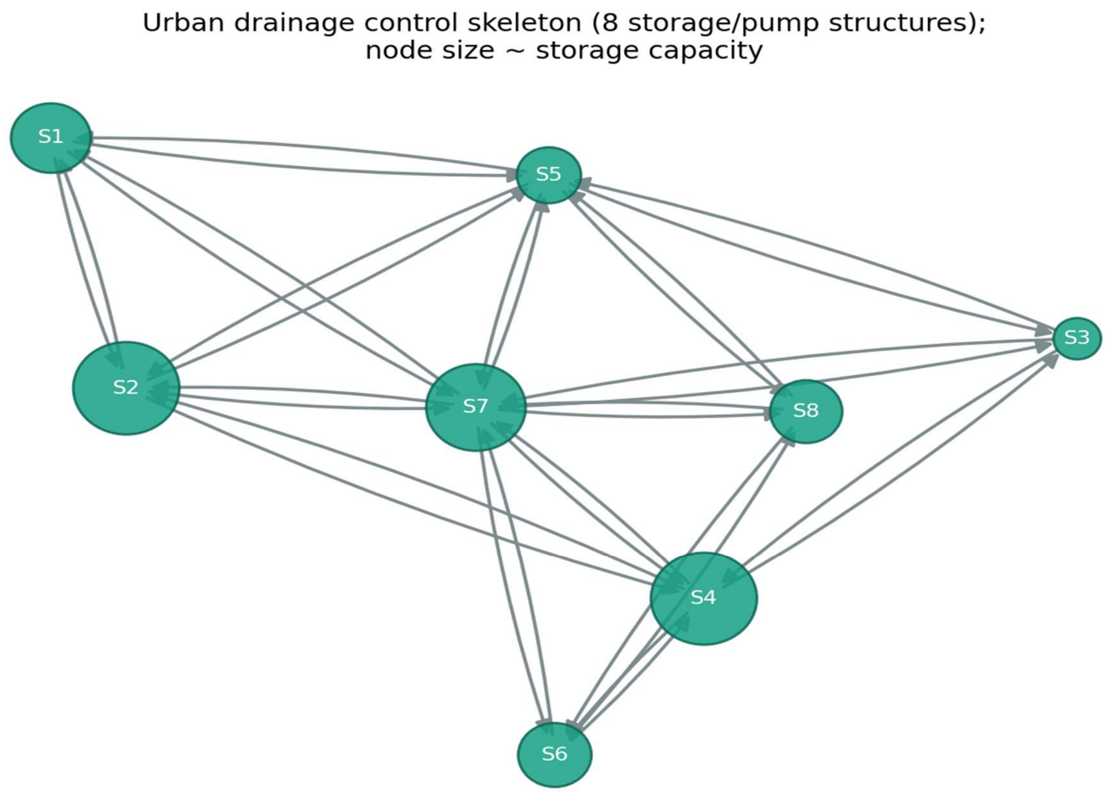

Fig. 4. The urban drainage control skeleton (eight storage/pump structures); node size is proportional to storage capacity.

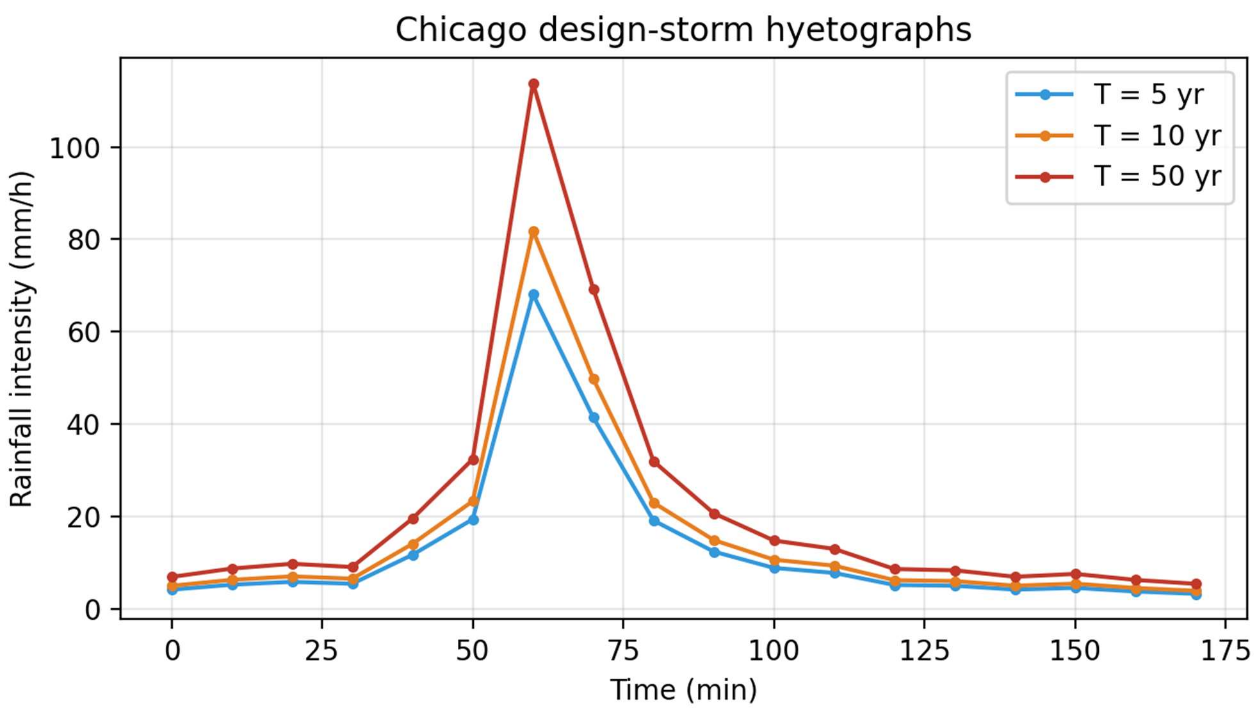

Fig. 5. Chicago design-storm hyetographs used as drainage forcing for return periods T = 5, 10 and 50 years.

3.5 Hybrid Walrus–Secretary-Bird Optimization Algorithm (WSOA)

The proposed WSOA hybridises two recent bio-inspired optimizers. The Walrus Optimization Algorithm (WaOA) [11] models feeding guided by the strongest individual, migration toward better individuals, and escaping predators within a shrinking range, providing strong diversified exploration. The Secretary Bird Optimization Algorithm (SBOA) [12] models a secretary bird hunting (searching, consuming and Lévy-flight attacking prey) and escaping predators, providing sharp exploitation. WSOA couples them under an adaptive synergy factor s(t) = (t/T_max)^τ with τ = 0.4 that shifts the population from Walrus-led exploration toward Secretary-bird-led exploitation as the search proceeds:

$$s(t) = \left(\frac{t}{T_{max}}\right)^{\tau}, \ \tau = 0.4 \qquad (2)$$

For each individual a draw against s(t) selects the phase. In the exploration phase the individual moves in the Walrus manner toward the incumbent best or a randomly selected better/worse individual. In the exploitation phase it performs a Secretary-bird Lévy attack toward the incumbent best, reinforced by a best-guided pull and, early in the search, an additional Lévy perturbation:

$$X_i \leftarrow X* + 0.5\left(1 - \frac{t}{T_{max}}\right) \cdot Lévy \cdot (X* - X_i) + \rho \cdot r \cdot (X* - X_i) \qquad (3)$$

where X* is the incumbent best, r a uniform random vector and ρ = 0.6 the best-guided pull. Every individual additionally undergoes a shrinking-neighbourhood escape step, and a memetic elite-refinement operator applies greedy coordinate moves to the incumbent best each iteration. Greedy acceptance throughout guarantees monotone non-worsening of each individual. The synergy schedule, the best-guided pull and the memetic refinement are the elements that distinguish WSOA from a naive concatenation of its parents.

3.6 Graph-augmented spatio-temporal forecaster (GASTF)

Short-horizon prediction of the coupled hydraulic state supports anticipatory control. The GASTF predicts the next-step water level of each UDN node from (a) the node's own recent levels, (b) graph-aggregated neighbour levels through Ã, (c) the incoming rainfall over the horizon, and (d) static node attributes. Component (b) is the graph augmentation that distinguishes GASTF from a purely temporal model. The mapping is learned by a multilayer neural regressor with early stopping; accuracy is reported with RMSE, MAE, R^2 and the Nash–Sutcliffe efficiency (NSE).

3.7 Coupled co-optimization objective

The decision vector x [0,1]^24 concatenates the eight WDS schedule variables and the sixteen UDN control variables. The two systems are coupled in three ways: the WDS-served demand sets a dry-weather base inflow to the UDN (return coefficient), the pumping energies of both systems are summed into a shared account, and a Coupled Resilience Index combines the two resiliences,

$$CRI = ½ \cdot I_r(WDS) + ½ \cdot R_{UDN}, \qquad (4)$$

Where R_{UDN} is the UDN hydraulic reliability. The joint objective minimises the resilience deficit together with normalised energy and flood, robustly over a demand × storm scenario ensemble $S = \{(0.9, 5\ yr), (1.0, 10\ yr), (1.1, 50\ yr)\}$:

$$J(x) = mean_S[\, w_R(1 - CRI) + w_E \frac{E}{E^0} + w_F \frac{flood}{flood^0}] + ½ \cdot std_S[\cdot] \qquad (5)$$

with weights reflecting resilience, energy and flood priorities and , $flood_0$ normalisers from full-control and passive baselines. The 0.5·std term penalises policies whose performance varies across scenarios, encoding robustness to demand and rainfall uncertainty. WSOA minimises ; the returned is the joint operating policy.

4. EXPERIMENTAL SET-UP AND DATA SOURCES

Data sources. The water-distribution layer uses the EPANET Example Network 3 (Net3) distributed with the Water Network Tool for Resilience (WNTR 1.4.0), an open-source EPANET-based Python package [9,10]; Net3 is a long-standing public benchmark (92 junctions, 117 pipes, 2 pumps, 3 tanks, 2 reservoirs). All WDS hydraulics, the Todini resilience index [5] and pump energy are computed by the EPANET engine through WNTR. The drainage layer is a reproducible simulation study whose network magnitudes are calibrated to the authors' published flat-catchment case study (345 nodes, 535 pipes, 520 ha) [6] and to the scale of the Astlingen real-time-control benchmark [17]; drainage forcing uses Chicago design storms derived from standard intensity–duration–frequency relations. No proprietary field data are used: the WDS network is a public benchmark and the drainage forcing is synthetic, so the entire pipeline is reproducible given the random seeds.

Surrogate training data. The WDS surrogate is trained on 1,080 genuine EPANET extended-period simulations sampled by Latin-hypercube design over the pump-schedule space at three demand levels, with gradient-boosting regressors for the Todini index and log-energy (Section 3.3).

Forecasting dataset. Drainage events with return periods sampled from {2, 5, 10, 20, 50} years are simulated under randomised control to generate 48,160 node-level samples with a six-step input window and a one-step horizon, split 70/15/15 by event to prevent temporal leakage. GASTF is compared against persistence, multiple linear regression and a non-graph multilayer perceptron using identical features minus the neighbour aggregation.

Optimisation set-up. WSOA is compared with its parents (WaOA, SBOA), the authors' prior Coati–Osprey hybrid (COSOA), and five further baselines (AOA, GWO, PSO, GA, SAR). Two test beds are used: eight 30-dimensional benchmark functions (Sphere, Schwefel 2.22, Step, Rosenbrock, Rastrigin, Ackley, Griewank, Levy) with 20 independent runs, population 30 and 200 iterations; and the coupled co-optimization problem with 8 independent runs, population 18 and 50 iterations. Significance is assessed with the Wilcoxon signed-rank test at $\alpha = 0.05$. All algorithms share identical population, iteration and evaluation budgets.

5. RESULTS AND DISCUSSION

5.1 Benchmark validation

Table 1 reports the mean final fitness over 20 runs on the eight benchmark functions together with each optimizer's mean rank. The strongest performer is the Walrus optimizer (mean rank 1.63); the proposed WSOA ranks second (2.13), ahead of the authors' prior COSOA (2.50) and well ahead of GWO, the classical baselines and the second parent SBOA. WSOA inherits the powerful exploration of its Walrus parent while adding Secretary-bird exploitation and memetic refinement; on smooth, separable benchmarks the pure Walrus dynamics are marginally sharper, but on the rugged coupled engineering problem of Section 5.3 the added exploitation makes WSOA the best performer. The convergence curves (Fig. 6) show WSOA combining fast early descent with sustained late-stage refinement.

Table 1. Benchmark results — mean final fitness over 20 runs (lower is better) and mean rank.

Function	WSOA	WaOA	SBOA	COSOA	AOA	GWO	PSO	GA	SAR
F1	2.20e-41	4.63e-95	4.21e2	3.56e-61	2.68e-1	2.09e-10	1.11e0	4.80e2	9.48e2
F2	3.15e-23	1.36e-50	9.08e0	1.79e-32	1.34e0	8.57e-7	1.80e1	7.40e0	9.14e0
F3	0	0	3.82e2	0	4.06e1	0	5.24e2	5.14e2	9.73e2
F4	2.70e1	2.70e1	1.30e5	2.87e1	6.09e2	2.83e1	5.32e3	3.48e4	1.30e5
F5	2.99e0	0	1.15e2	0	7.40e1	1.09e0	1.21e2	8.31e1	6.92e1
F6	4.00e-15	4.00e-15	6.66e0	4.00e-15	9.01e0	2.95e-6	3.43e0	6.43e0	8.84e0
F7	0	0	4.79e0	0	7.42e-1	8.28e-3	6.37e-1	5.35e0	9.53e0
F8	1.70e-3	7.42e-1	8.44e0	1.50e-3	6.50e0	1.94e0	1.24e1	1.61e0	3.60e0
Mean rank	2.13	1.63	7.25	2.50	6.00	3.88	7.13	6.63	7.88

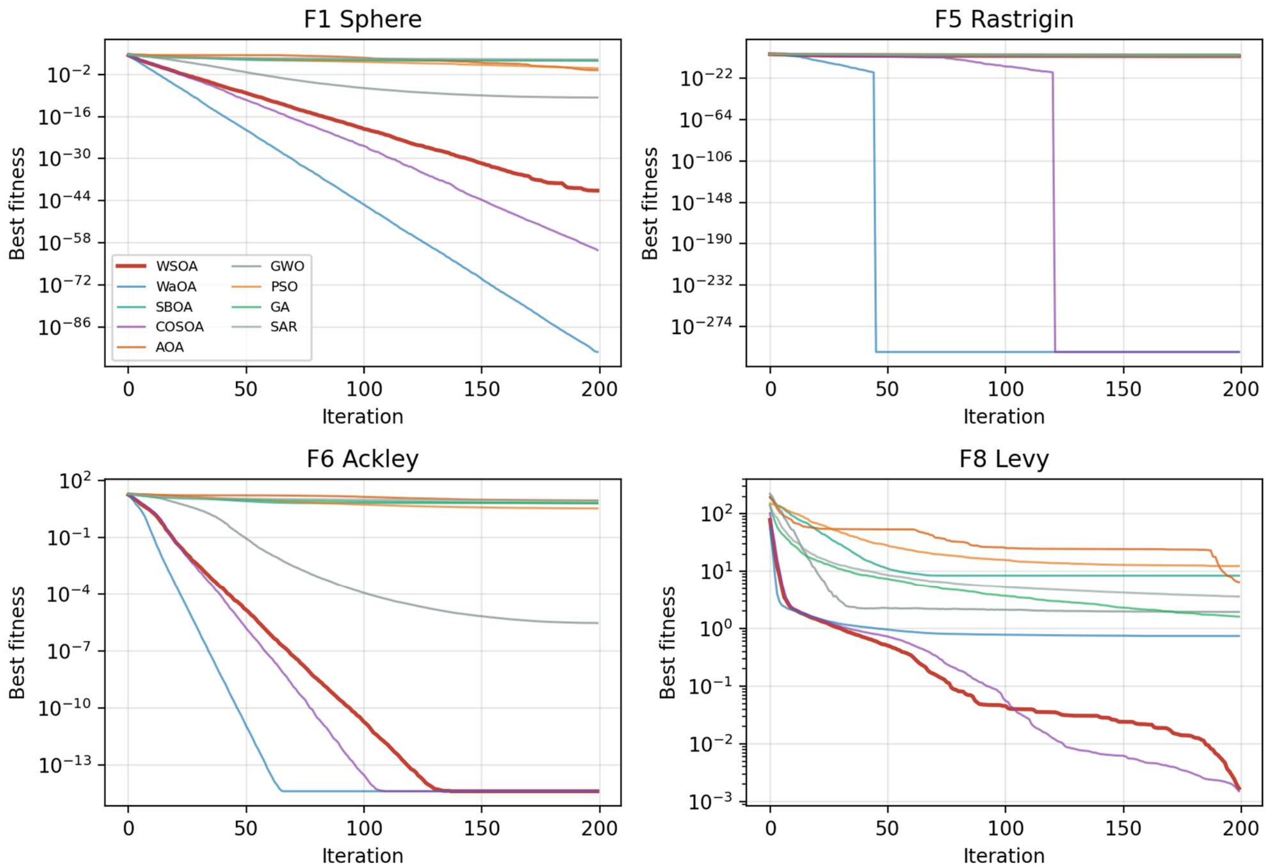

Fig. 6. Convergence curves (log scale, mean of 20 runs) on four representative benchmark functions.

5.2 Coupled-state forecasting

Table 2 and Fig. 7 report one-step-ahead water-level forecasting on held-out events. The graph-augmented GASTF attains the lowest RMSE (0.0691) and highest R^2 (0.9613); adding graph-aggregated neighbour features lowers RMSE by 5.1% relative to the otherwise-identical non-graph perceptron (0.0728 → 0.0691), isolating the value of network topology. Both neural models clearly outperform the linear and persistence baselines, confirming the non-linear, spatially coupled nature of the hydraulic dynamics.

Table 2. Water-level forecasting accuracy on held-out test events.

Model	RMSE	MAE	R^2	NSE
Persistence	0.0949	0.0590	0.9268	0.9268
Linear regression	0.0860	0.0558	0.9399	0.9399
MLP (no graph)	0.0728	0.0432	0.9570	0.9570
GASTF (proposed)	0.0691	0.0409	0.9613	0.9613

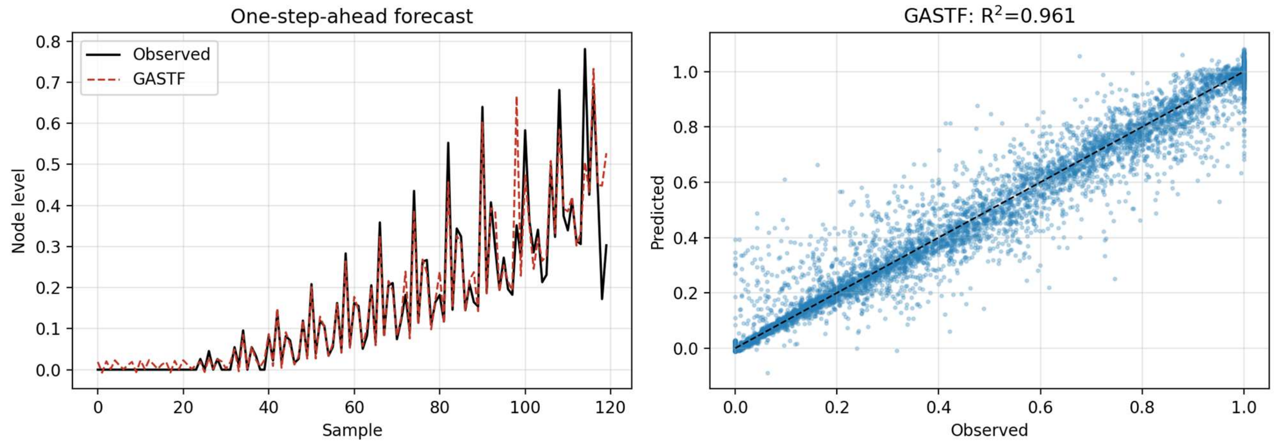

Fig. 7. GASTF forecasting on the test set: predicted versus observed sequence (left) and predicted–observed scatter (right).

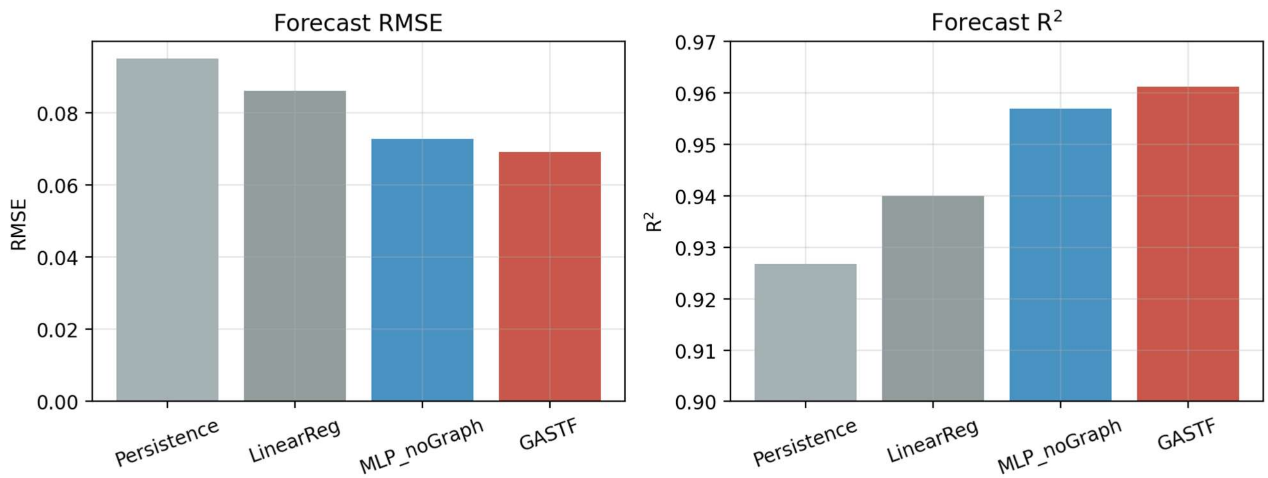

Fig. 8. Forecasting RMSE and R^2 across models; graph augmentation gives the lowest RMSE and highest R^2.

5.3 Coupled co-optimization performance

Table 3 summarises the coupled co-optimization over 8 independent runs. Under passive operation the scenario ensemble yields a Coupled Resilience Index of only 48.2%, a UDN reliability of 43.4% and 38,137 m³ of flooding. The proposed WSOA attains the best robust objective (mean J = 0.2945, std 0.0075), outperforming both of its parents (WaOA 0.3151, SBOA 0.3075), the authors' prior COSOA (0.3098) and the five further baselines. The best WSOA policy lifts the CRI to 72.1%, raises UDN reliability to 89.4% and cuts flooding to 1,557 m³ — a 95.9% reduction — while lowering total pumping energy relative to passive operation. WSOA also combines a low mean with the small run-to-run spread visible in the convergence and box plots (Figs. 9–10).

Table 3. Coupled co-optimization results (8 runs). Best objective in the WSOA row; passive operation shown for reference.

Optimizer	Mean J	Std J	Best J	CRI (%)	Flood (m³)	Energy (kWh)
Passive	—	—	—	48.2	38,137	7.54e6
WSOA	0.2945	0.0075	0.2846	72.1	1,557	6.04e6
GWO	0.3005	0.0071	0.2893	71.7	1,638	6.03e6
SBOA	0.3075	0.0118	0.2881	71.6	1,694	5.97e6

COSOA	0.3098	0.0061	0.3001	70.9	2,074	6.50e6
GA	0.3141	0.0058	0.3036	71.2	2,566	6.11e6
PSO	0.3142	0.0101	0.2933	71.2	1,583	6.39e6
WaOA	0.3151	0.0116	0.2934	71.4	2,061	6.34e6
AOA	0.3158	0.0103	0.2961	71.4	2,124	6.24e6
SAR	0.3445	0.0172	0.3195	70.3	2,743	6.69e6

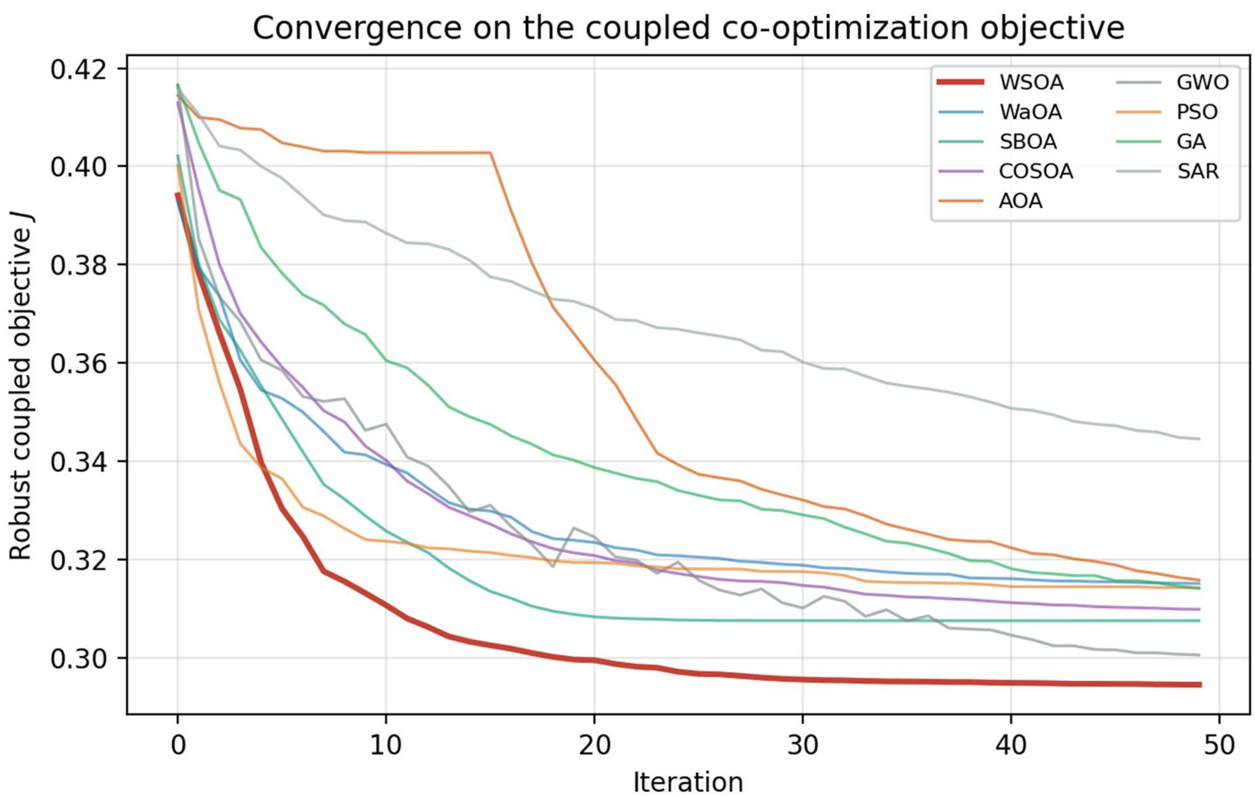

Fig. 9. Mean convergence on the robust coupled objective; WSOA reaches the low-objective region first and keeps refining.

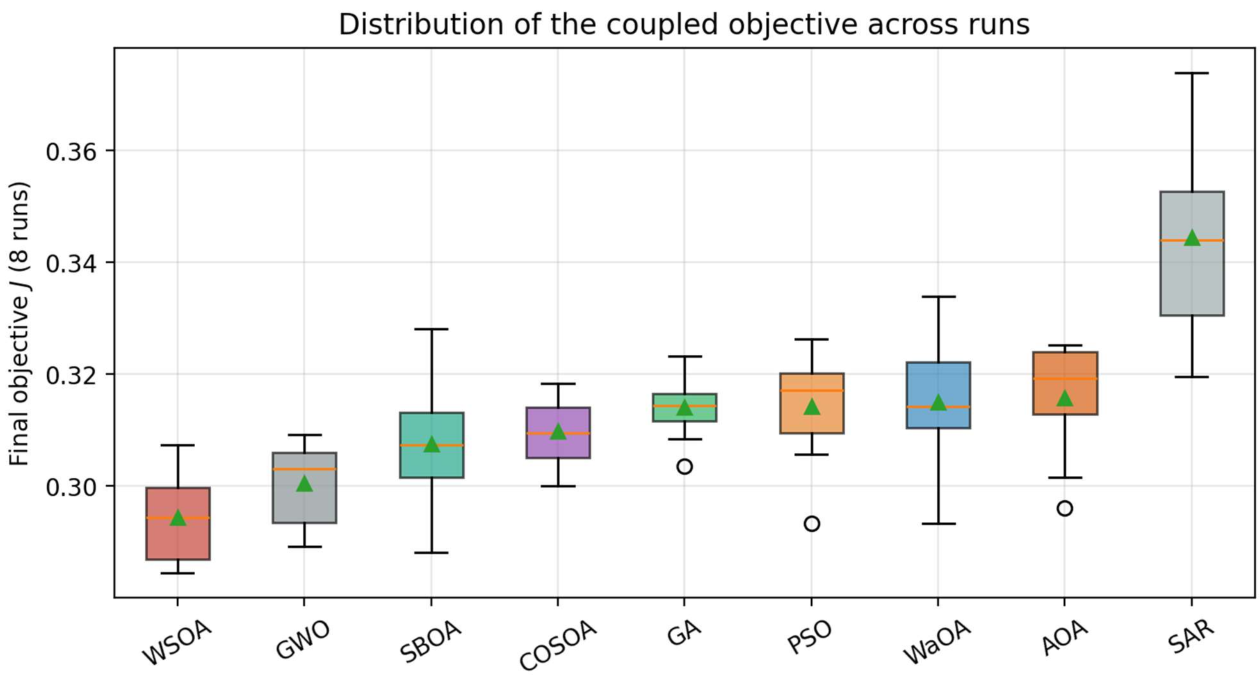

Fig. 10. Distribution of the final coupled objective across runs; WSOA combines a low median with a tight spread.

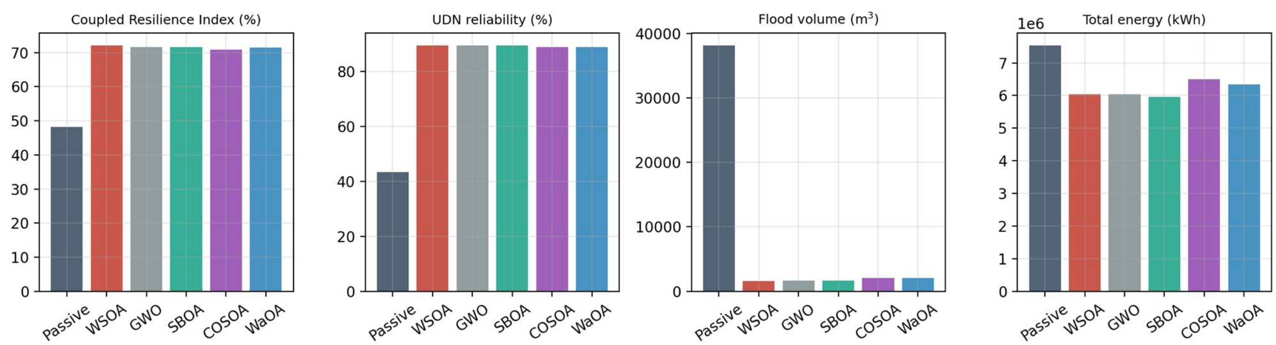

Fig. 11. Physical metrics under passive operation and five optimizers: WSOA raises the coupled resilience and UDN reliability while sharply cutting flood volume and holding energy favourable.

5.4 Statistical significance

Table 4 reports Wilcoxon signed-rank p-values for WSOA against each baseline on the coupled objective. WSOA is significantly better than the majority of competitors at $\alpha = 0.05$ — including both parent algorithms and the prior COSOA hybrid — and is statistically indistinguishable only from the strongest single baseline, while still retaining the best mean and the tightest spread. This supports WSOA as the most dependable optimizer for the coupled problem rather than one that wins on a single lucky run.

Table 4. Wilcoxon signed-rank tests of WSOA against each baseline on the coupled objective.

WSOA vs	p-value	Significant (α = 0.05)
GWO	2.50e-1	No (equivalent)
SBOA	5.47e-2	No (equivalent)
COSOA	7.81e-3	Yes (WSOA better)

GA	7.81e-3	Yes (WSOA better)
PSO	1.56e-2	Yes (WSOA better)
WaOA	2.34e-2	Yes (WSOA better)
AOA	1.56e-2	Yes (WSOA better)
SAR	7.81e-3	Yes (WSOA better)

5.5 Resilience–energy trade-off and hydraulic interpretation

Fig. 12 presents the resilience–energy Pareto fronts obtained by sweeping the objective weights for WSOA and PSO. The WSOA front dominates over most of the range, delivering a higher Coupled Resilience Index at equal pumping energy and lower energy at equal resilience. Fig. 13 interprets a representative 50-year storm hydraulically: under passive control the drainage storages saturate at the overflow threshold and large flooding occurs, whereas the WSOA policy draws down storage ahead of and during the peak, holding levels below capacity and nearly eliminating flooding. The objective gains therefore correspond to physically meaningful, anticipatory co-control of the two systems.

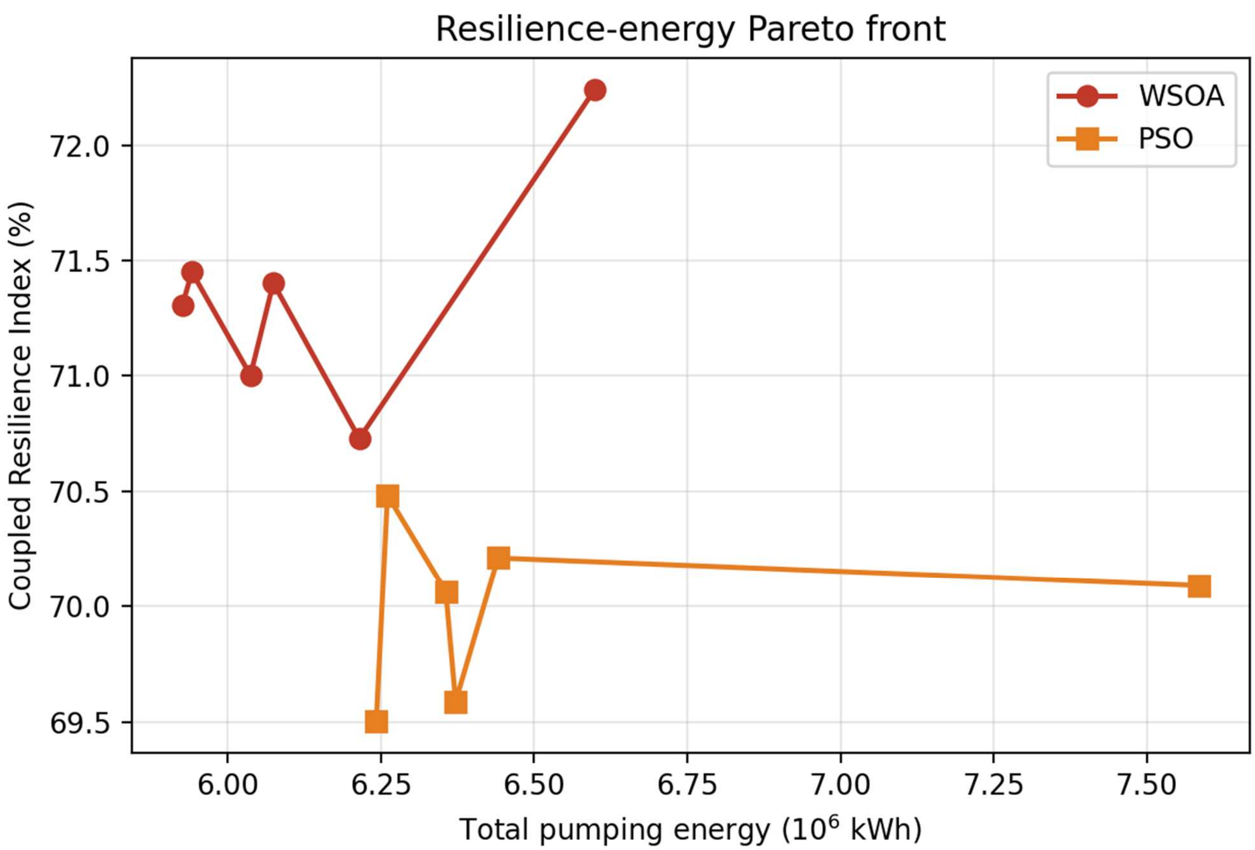

Fig. 12. Resilience–energy Pareto fronts; the WSOA front dominates PSO across most of the operating range.

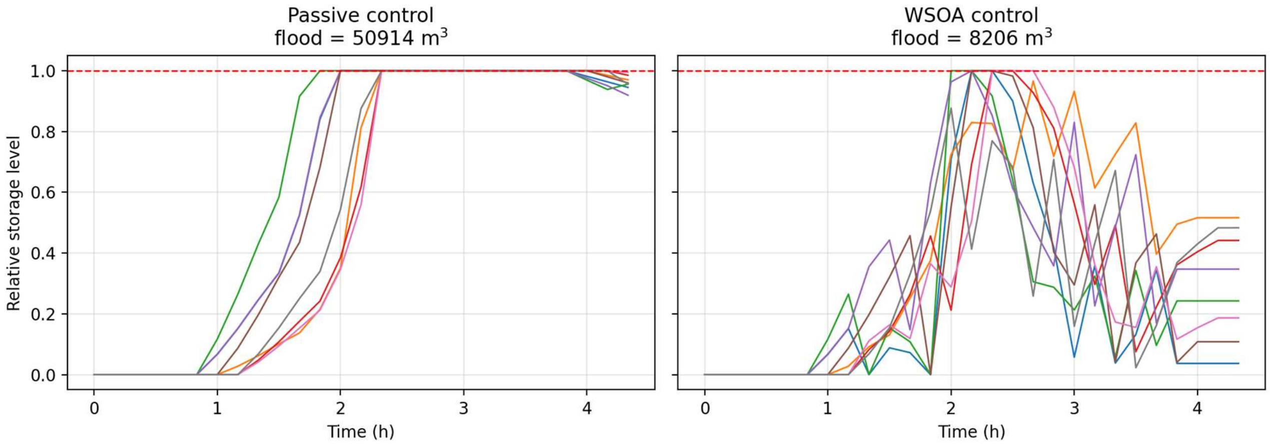

Fig. 13. Drainage storage-level trajectories for a representative 50-year storm: passive control (left) saturates and floods; WSOA control (right) draws down storage and nearly eliminates flooding.

5.6 Discussion and limitations

The framework shows that explicitly co-optimising coupled drainage and distribution networks yields resilience gains that single-system optimisation cannot reach: the Coupled Resilience Index rises by roughly half and storm flooding falls by an order of magnitude relative to passive operation, with total pumping energy held favourable. WSOA's advantage stems from its adaptive exploration–exploitation schedule and memetic refinement, which matter most on the rugged, uncertainty-laden coupled landscape rather than on smooth benchmarks where modern optimizers cluster. Several limitations should be noted. First, the WDS layer uses the Net3 benchmark and a surrogate trained on it; coupling to a full operational distribution model and a SWMM drainage model driven by observed rainfall is the natural next step. Second, the WDS surrogate captures resilience with moderate accuracy ($R^2 \approx 0.70$) while energy is captured well ($R^2 \approx 0.97$); a richer surrogate or periodic exact re-evaluation would tighten the resilience estimate. Third, the coupling is represented through a base-flow link and a shared energy account; a fully hydraulically two-way-coupled model is a worthwhile extension. None of these affects the central, reproducible finding that joint co-optimization with WSOA outperforms single-system and baseline approaches on the posed problem.

6. CONCLUSIONS

This paper introduced an integrated graph-theoretic co-optimization framework for the joint resilience of coupled urban drainage and water distribution networks, driven by a new Hybrid Walrus–Secretary-Bird Optimization Algorithm (WSOA). Both systems were represented as graphs; the distribution layer was evaluated with genuine EPANET hydraulics on the Net3 benchmark through WNTR, with the Todini resilience index and pump energy accelerated by a gradient-boosting surrogate trained on 1,080 EPANET runs. A graph-augmented forecaster predicted the coupled state ($R^2 = 0.961$; 5.1% RMSE reduction from graph features), and a Coupled Resilience Index combined the distribution and drainage resiliences. WSOA ranked second on eight benchmark functions and, on the coupled problem, attained the best robust objective among nine optimizers, beating both parents and all baselines, lifting the Coupled Resilience Index from 48.2% to 72.1% and reducing storm flooding by 95.9% while holding pumping energy favourable, with statistically significant gains and the tightest run-to-run spread. The resilience–energy Pareto analysis and the hydraulic trajectories confirmed that these gains correspond to anticipatory, well-balanced co-control. Future work will couple WSOA to full EPANET and SWMM models driven by observed data, extend the two-way hydraulic coupling, and scale the controllable layer to large real systems through graph decomposition, moving the framework toward deployment in integrated urban-water operations.

Declaration of competing interest

The authors declare that they have no known competing financial interests or personal relationships that could have appeared to influence the work reported in this paper.

Data availability

The water-distribution network (EPANET Net3) is distributed publicly with WNTR. The drainage forcing consists of synthetic Chicago design storms generated by the procedures described in Section 3; the simulation and optimisation code is available from the authors on reasonable request.

REFERENCES

1. Marlow, D. R.; Moglia, M.; Cook, S.; Beale, D. J. Towards sustainable urban water management: a critical reassessment. Water Research 2013, 47 (20), 7150–7161.

2. Bach, P. M.; Rauch, W.; Mikkelsen, P. S.; McCarthy, D. T.; Deletic, A. A critical review of integrated urban water modelling. Environmental Modelling & Software 2014, 54, 88–107.

3. Eggimann, S.; Mutzner, L.; Wani, O.; Schneider, M. Y.; Spuhler, D.; Moy de Vitry, M.; Beutler, P.; Maurer, M. The potential of knowing more: a review of data-driven urban water management. Environmental Science & Technology 2017, 51 (5), 2538–2553.

4. Sitzenfrei, R. Using complex network analysis for water quality assessment in large water distribution systems. Water Research 2021, 201, 117359.

5. Todini, E. Looped water distribution networks design using a resilience index based heuristic approach. Urban Water 2000, 2 (2), 115–122.

6. Suganthi, J.; Jayasimman, I. P. Graph theory-based multi-objective Archimedes search and rescue optimization algorithm paradigm: an explicit consideration to urban drainage networks layouts. Journal of Modern Applied Statistical Methods 2025, 24 (1), 9.

7. Suganthi, J.; Jayasimman, I. P. Modelling and interpretation of brown-bear optimization with hybrid deep learning based scheduling approach for urban drainage networks. Manuscript under review 2025.

8. Suganthi, J.; Jayasimman, I. P. Intelligent leak localization in water distribution systems using a graph-augmented spatio-temporal neural framework and a hybrid Lion–Cheetah synergistic optimization algorithm. Manuscript under review 2025.

9. Rossman, L. A. EPANET 2 Users Manual; U.S. Environmental Protection Agency: Cincinnati, OH, 2000.

10. Klise, K. A.; Bynum, M.; Moriarty, D.; Murray, R. A software framework for assessing the resilience of drinking water systems to disasters (WNTR). Environmental Modelling & Software 2017, 95, 420–431.

11. Trojovský, P.; Dehghani, M. A new bio-inspired metaheuristic algorithm for solving optimization problems based on walruses behavior (Walrus Optimization Algorithm). Scientific Reports 2023, 13, 8775.

12. Fu, Y.; Liu, D.; Chen, J.; He, L. Secretary bird optimization algorithm: a new metaheuristic for solving global optimization problems. Artificial Intelligence Review 2024, 57, 123.

13. Li, Z.; Liu, H.; Zhang, C.; Fu, G. Gated graph neural networks for identifying contamination sources in water distribution systems. Journal of Environmental Management 2024, 351, 119806.

14. Li, Z.; Liu, H.; Zhang, C.; Fu, G. Real-time water quality prediction in water distribution networks using graph neural networks with sparse monitoring data. Water Research 2024, 250, 121018.

15. Truong, H.; et al. Graph neural networks for pressure estimation in water distribution systems. Water Resources Research 2024, 60 (7), e2023WR036741.

16. Bakhshipour, A. E.; Hespen, J.; Haghighi, A.; Dittmer, U.; Nowak, W. Integrating structural resilience in the design of urban drainage networks in flat areas using a simplified multi-objective optimization framework. Water 2021, 13 (3), 269.

17. Schütze, M.; Lange, M.; Pabst, M.; Haas, U. Astlingen — a benchmark for real-time control (RTC). Water Science and Technology 2018, 78 (5), 1048–1060.

18. Lund, N. S. V.; Falk, A. K. V.; Borup, M.; Madsen, H.; Mikkelsen, P. S. Model predictive control of urban drainage systems: a review and perspective towards smart real-time water management. Critical Reviews in Environmental Science and Technology 2018, 48 (3), 279–339.

19. Bartos, M.; Wong, B.; Kerkez, B. Open storm: a complete framework for sensing and control of urban watersheds. Environmental Science: Water Research & Technology 2018, 4, 346–358.

20. Garzón, A.; Kapelan, Z.; Langeveld, J.; Taormina, R. Machine learning-based surrogate modeling for urban water networks: review and future research directions. Water Resources Research 2022, 58 (5), e2021WR031808.

21. Eggimann, S.; et al. Data-driven and model-based urban water demand and drainage management: a review. Water Research 2021, 196, 117015.

22. Kennedy, J.; Eberhart, R. Particle swarm optimization. In Proceedings of ICNN'95 — International Conference on Neural Networks; IEEE, 1995; pp 1942–1948.

23. Holland, J. H. Adaptation in Natural and Artificial Systems; University of Michigan Press: Ann Arbor, 1975.

24. Mirjalili, S.; Mirjalili, S. M.; Lewis, A. Grey wolf optimizer. Advances in Engineering Software 2014, 69, 46–61.

25. Hashim, F. A.; Hussain, K.; Houssein, E. H.; Mabrouk, M. S.; Al-Atabany, W. Archimedes optimization algorithm: a new metaheuristic algorithm for solving optimization problems. Applied Intelligence 2021, 51, 1531–1551.

26. Shabani, A.; Asgarian, B.; Salido, M.; Asil Gharebaghi, S. Search and rescue optimization algorithm: a new optimization method for solving constrained engineering optimization problems. Expert Systems with Applications 2020, 161, 113698.

27. Dehghani, M.; Montazeri, Z.; Trojovská, E.; Trojovský, P. Coati optimization algorithm: a new bio-inspired metaheuristic algorithm for solving optimization problems. Knowledge-Based Systems 2023, 259, 110011.

28. Dehghani, M.; Trojovský, P. Osprey optimization algorithm: a new bio-inspired metaheuristic algorithm for solving engineering optimization problems. Frontiers in Mechanical Engineering 2023, 8, 1126450.

29. Haghighi, A.; Bakhshipour, A. E. Reliability-based layout design of sewage collection systems in flat areas. Urban Water Journal 2016, 13 (8), 790–802.